

# Tracking Any Object Amodally

Cheng-Yen (Wesley) Hsieh<sup>1</sup>Tarasha Khurana<sup>1</sup>Achal Dave<sup>2</sup>Deva Ramanan<sup>1</sup><sup>1</sup>Carnegie Mellon University <sup>2</sup>Toyota Research Institute<https://tao-amodal.github.io>

Figure 1. **Representative sequences of our TAO-Amodal dataset.** Our dataset augments the TAO dataset [10] with amodal bounding box annotations for fully invisible, out-of-frame, and occluded objects. Note that this implies TAO-Amodal also includes modal segmentation masks (as visualized in the color overlays above). Our dataset encompasses 880 categories, aimed at assessing the occlusion reasoning capabilities of current trackers through the paradigm of Tracking Any Object with Amodal perception (TAO-Amodal).

## Abstract

*Amodal perception, the ability to comprehend complete object structures from partial visibility, is a fundamental skill, even for infants. Its significance extends to applications like autonomous driving, where a clear understanding of heavily occluded objects is essential. However, modern detection and tracking algorithms often overlook this critical capability, perhaps due to the prevalence of modal annotations in most datasets. To address the scarcity of amodal data, we introduce the TAO-Amodal benchmark, featuring 880 diverse categories in thousands of video sequences. Our dataset includes amodal and modal bounding boxes for visible and occluded objects, including objects that are partially out-of-frame. To enhance amodal tracking with object permanence, we leverage a lightweight plug-in module, the amodal expander, to transform standard, modal trackers into amodal ones through fine-tuning on a few hundred video sequences with data augmentation. We achieve a 3.3% and 1.6% improvement on the detection and tracking of occluded objects on TAO-Amodal. When evaluated on people, our method produces dramatic improvements of 2x compared to state-of-the-art modal baselines.*

## 1. Introduction

Machine perception, particularly in object detection and tracking, has focused primarily on reasoning about *visible* or modal objects. This modal perception ignores parts of the three-dimensional world that are *occluded* to the camera. However, amodal completion of objects in the real-world (e.g., seeing a setting sun but understanding it is whole) and their persistence over time (e.g., person walking behind a car in Fig. 2) are fundamental capabilities that develop in humans in their early years [3, 28, 43]. In autonomous systems, this online amodal reasoning finds a direct application in downstream motion planning and navigation. Despite this, object detection and tracking stacks give little importance to partially or completely occluded objects; this becomes apparent in datasets that are only annotated modally [9, 10, 15, 16, 21, 31, 32, 38, 57, 61] but are still widely used and built upon by algorithms. These algorithms [12, 17, 25, 34, 36, 37, 41, 46, 64] in turn learn to perceive only modal objects.

To address this gap, we first introduce a benchmark for large-scale amodal tracking, which requires estimating the full extent of objects through heavy and even complete occlusions. Our benchmark annotates 17,000 objects with

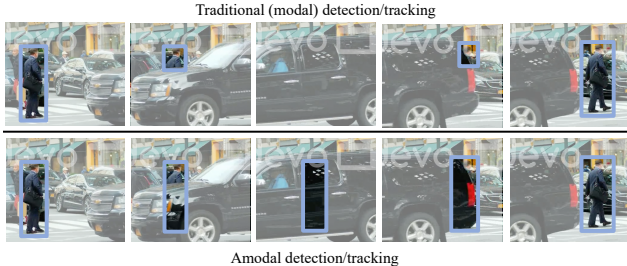


**Figure 2. Traditional modal perception (top) vs. amodal perception (bottom).** Given a sequence of images, traditional detection and tracking algorithms concentrate on identifying visible segments of multiple objects within the scene. Consequently, they face challenges resulting in peculiar output such as vanishing bounding boxes or tiny box sizes under occlusion scenarios. Amodal perception advances beyond conventional approaches by inferring complete object boundaries, thereby predicting bounding boxes that extend to the full object extent, even when certain portions are occluded.

amodal bounding boxes, along with human confidence estimates, from 880 classes in 2,921 videos. While prior datasets focus on images or are limited to a small vocabulary of classes (Tab. 1), our benchmark evaluates amodal tracking for hundreds of object classes. Since objects can get occluded because of other objects in the scene, *and* because of the limited field-of-view of cameras in casual captures, we define and address two kinds of occlusions – in-frame, and out-of-frame. As annotating amodal bounding boxes can be ambiguous and challenging, we design a new annotation protocol with detailed guidelines to improve human annotation. Importantly, we base our benchmark on a large-vocabulary multi-object tracking dataset, TAO [10]. This choice allows us to pair our amodal box annotations with class labels, modal boxes, and precise modal mask annotations [2] collected in prior work.

Equipped with this data, we set out to evaluate the difficulty of amodal tracking. We evaluate using standard metrics, including detection and tracking AP, and variants that evaluate tracking specifically under partial and complete occlusions. As expected, we find that standard trackers trained with modal annotations do not suffice for amodal tracking.

We present an effective module to turn modal trackers into amodal trackers with object permanence. Specifically, we build a class-agnostic amodal expander, inspired by [65], that expands modal bounding box predictions to cover the full extent of objects. With limited amodal training data, we build the amodal expander to be class-agnostic, allowing us to transfer across classes for which we have fewer amodal annotations. Specifically, for amodal detection of people, we observe dramatic relative improvements of  $\sim 30.0$  AP points as compared to modal baselines. Our results show strong improvements over state-of-the-art

trackers for amodal tracking.

In summary, our contributions are as follows: (1) We annotate a large-scale dataset of amodal tracks for diverse objects, consisting of 17k objects spanning 880 categories, (2) we adapt evaluation metrics to handle amodal settings, and evaluate state-of-the-art trackers for our new task, and finally, (3) we present a strong baseline for amodal tracking with object permanence, using a category-agnostic amodal expander module.

## 2. Related work

Amodal perception has been studied in the past by benchmarks and algorithms, in both the single-frame (detection) and multi-frame (detection and tracking) settings. Since amodal object annotations are hard to obtain due to the uncertainty in human annotations (c.f. prior work [30] on a human vision experiment), the community has seen more dependence either on synthetic datasets, or real-world datasets with few classes and limited diversity. The remainder of the sections talk about this in detail.

### 2.1. Benchmarks

**Real-world datasets** In the surveillance and self-driving domains, real-world datasets that annotate objects amodally exist. MOT 15-20 [11, 33, 42] evaluate multi-object tracking on amodal person detections obtained from detectors trained on MOT annotations. One pitfall for MOT is that instead of humans labelling the boxes during “invisible” phases of people, these box annotations are just linearly interpolated between two visible frames of the same object. Additionally, the metrics used by MOT weigh all modal and amodal annotations equally. This downweights the tracking performance on amodal objects as they form only a small fraction of all annotations.

A number of multimodal (images and 3D LiDAR) datasets for autonomous driving have recently become popular. These include ArgoVerse (1.0 and 2.0) [7, 58], Waymo [50], nuScenes [5] and KITTI [18]. These datasets aim to focus on 3D tasks, and therefore use human annotators to label all objects in 3D to their full extent. In this setting, amodal perception is organic, and almost trivial, as in a fully-3D world there are no occlusions. These 3D boxes when projected onto 2D images would be useful for amodal perception but unfortunately, they only cover a small number of object classes. Another way to obtain amodal object annotations is in a multi-view setting. Datasets like CarFusion [45] and MMPTTrack [22] follow this data curation scheme but because of the cumbersome data collection process, they are limited to only a single or few categories.

In the single-frame setting, COCO-Amodal, Amodal KINS and NuImages [5, 44, 65] contain amodal annotations of a few objects, but only cover the cases of partial occlusion (as complete occlusion is hard to resolve

|                   | # Sequences |            |             |            | # Occluded Boxes |               |             | # Occluded tracks | Track length | Ann fps   | Total length  |
|-------------------|-------------|------------|-------------|------------|------------------|---------------|-------------|-------------------|--------------|-----------|---------------|
|                   | Train       | Val        | Test        | Classes    | Partial          | Heavy         | OoF         |                   |              |           |               |
| COCO-Amodal [65]  | 2500        | 1250       | 1250        | -*         | 8.8k             | 0.2k          | 0           | -                 | -            | -         | -             |
| Sail-VOS [26]     | 160         | 41         | 0           | 162        | 559.5k           | 704.8k        | 0           | 7.9k              | 14.14        | 8         | 3,359         |
| Sail-VOS-3D [27]  | 161         | 41         | 0           | 24         | 295.0k           | 387.5k        | 0           | 5.0k              | 13.10        | 8         | 2,808         |
| NuScenes [5]      | <b>700</b>  | 150        | 150         | 23         | 571.1k           | <b>139.5k</b> | <b>219k</b> | <b>24.5k</b>      | 9.06         | 20        | 6,000         |
| MOT17 [42]        | 7           | 0          | 7           | 1          | 51.2k            | 16.4k         | 16k         | 0.1k              | 6.98         | <b>30</b> | 248           |
| MOT20 [11]        | 4           | 0          | 4           | 1          | <b>729.4k</b>    | 88.1k         | 88k         | 1.6k              | 20.55        | 25        | 178           |
| <b>TAO-Amodal</b> | 500         | <b>993</b> | <b>1428</b> | <b>880</b> | 158.2k           | 35.1k         | 139k        | 9.6k              | <b>22.24</b> | 1         | <b>88,605</b> |

Table 1. **Statistics of amodal datasets.** We compare TAO-Amodal to prior image (first block), synthetic video (second block), and real video (last block) datasets. Compared to existing amodal datasets, TAO-Amodal is notable for being *real-world* videos that span far *more categories* and far *more annotated frames* for evaluation. We define heavy occlusion as objects with visibility below 10%, and partial as between 10%-80%. Occluded tracks are those that have heavy or partial occlusions for more than 5 seconds. Out-of-frame (OoF) objects are ones that extend partially beyond the image boundary. Track length is averaged over the dataset in seconds, while total length is the length of eval sequences in seconds.

in a single-frame setting without temporal visibility cues). Moreover, COCO-Amodal [65] and Amodal KINS [44] are not shipped with class labels, which makes it difficult to learn object-specific priors for amodal completion.

**Synthetic datasets** Intuitively, it is cheap to get amodal object annotations from synthetic data setups. SAIL-VOS and SAILVOS-3D [26, 27] are such datasets that exploit synthetic dataset curation and come with a number of different types of annotations (bounding boxes, object masks, object categories, their long-range tracks, and 3D meshes). Some of these even suit our case of detecting ‘out-of-frame’ occlusions, where one could project 3D meshes onto the image plane. While the number of categories are slightly larger for these datasets (including others like ParallelDomain [53] and DYCE [14]), the sim-to-real transfer remains a challenge even for modal perception [8, 29].

## 2.2. Algorithms

Based off of some amodal datasets, there has been a growing interest in developing algorithms suitable for amodal perception. Some methods aim to track objects with object permanence [30, 53–55]. Some approaches utilize prior-frame information [4, 6, 13, 49, 59, 60, 63]. For instance, GTR [53] employs a transformer-based architecture and uses trajectory queries to group bounding boxes into trajectories. Previous work also segment objects amodally [35, 39]. We lean on similar approaches in this work, and devise a mechanism to generate occlusion cases in the flavor of the data augmentation used by GTR [64], and show that this is essential to the goal of enabling amodal perception.

## 3. Dataset Annotation

**Base dataset.** Existing datasets for modal perception are limited either in terms of their diversity, or the vocabulary of classes labelled. To this end, we build upon the modally annotated TAO dataset. It contains bounding box track annotations of 833 object categories at 1FPS spanning a total of 2,921 videos from 7 different data sources (AVA [20], Argoverse [7], Charades [47], HACS [62], LaSOT [16], BDD100K [61], YFCC100M [52]). This gives us the advantage of adding amodal box annotations to an already existing set of multimodal annotations in TAO (i.e., object classes, modal bounding boxes and modal segmentation masks). In terms of the extent/scope of annotation, TAO follows the single-frame detection datasets like LVIS and OpenImages [21, 31], in adopting a federated annotation protocol for object tracking, i.e., not every object is exhaustively annotated in every video. For collecting amodal annotations in TAO-Amodal, we consider only the set of tracks that are labelled in TAO.

**Scope.** Since annotators can exhibit a large variation in annotating the precise shape of objects while they undergo partial or even complete occlusion, we annotate using bounding boxes (instead of segmentation masks like in BURST [2]) to annotate their extent in the visible scene. Additionally, we define ‘in-frame’ occlusions as those occurring from the presence of occluders (occluders might be other dynamic objects, or static scene elements), and ‘out-of-frame’ occlusions as those resulting from objects leaving the camera field-of-view. We do not label the extent of occlusion in cases where an object may be partially present behind the camera (e.g., a person holding the camera who has their hands visible in the image). For labelling ‘out-

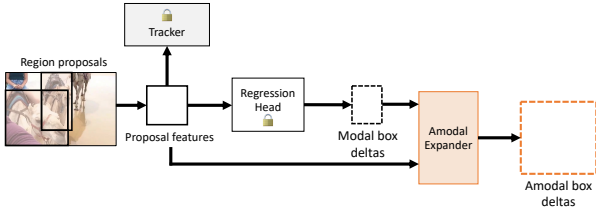


Figure 3. **ROI Head [19] with Amodal Expander.** Our Amodal Expander serves as a plug-in module that can “amodalize” any existing detector or tracker with limited (amodal) training data. It operates by taking as input region proposal features and modal box predictions (often represented as a residual delta with respect to the region proposal) and generates amodal box outputs (again represented as residual deltas). To enable learning from limited data, we freeze all modules except the amodal expander.

of-frame’ occlusions, we need to fix bounds for annotation on the image plane. We ask annotators to work within an *annotation workspace* that extends to twice the image dimensions in consideration, with the image itself horizontally and vertically center-aligned in this workspace.

**Annotation Protocol** Since TAO tracks (and their individual bounding boxes) are modal in nature, extending boxes to account for in-frame and out-of-frame occlusions translates to (1) modifying existing boxes in TAO, for the cases of partial occlusion, and (2) adding new boxes for completely occluded objects. We find that out of a total of 358,862 boxes in TAO, 266,902 (74.4%) boxes are modified to incorporate partial occlusion. TAO-Amodal boasts of an additional 23,449 bounding boxes for invisible objects that were not in TAO. These annotations follow the guidelines detailed in the appendix, that cover a wide range of both in-frame and out-of-frame occlusion scenarios. Importantly on a higher-level, we only consider the occlusion cases, where an object has appeared in the scene before. We also scope out the occlusion cases, where an object might be partially behind the camera, or outside the annotation workspace defined above. Within the strict purview of the guidelines, when an object’s location cannot be discerned confidently by the annotators, an `is_uncertain` flag is added to the labeled bounding box. From the 23,449 boxes for invisible objects, 20,218 (85.8%) boxes are annotated confidently (i.e., without the uncertain flag), indicating that there is inherent uncertainty in localizing objects when they undergo heavy occlusions (ref. human vision experiment from a prior work [30]).

Finally, equipped with both modal and amodal annotations for all objects in TAO and TAO-Amodal, we add a visibility field to the TAO-Amodal annotations. From qualitative visual inspection, we find that the IoU between the modal and amodal boxes, is a good enough approximation

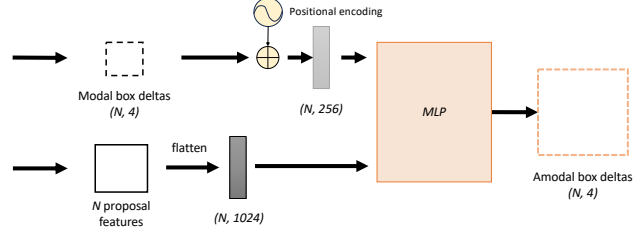


Figure 4. **Amodal Expander Architecture.** Given  $N$  flattened proposal features and modal box (delta) predictions represented with 256-dim positional encodings [56], we predict amodal box (deltas) with a two-layer MLP (unless otherwise specified). Further architecture details could be found in Sec. 5.2

of the visibility of each object.

**Quality Control** We ensure two rounds of professional quality check on TAO-Amodal annotations; this means all bounding box annotations are refined twice by annotators. Finally, authors conduct a manual quality check where 7 videos are chosen at random from the 7 dataset subsets and only 2 out of 349 tracks are found to be erroneous. These are tracks of invisible objects (visibility 0.0%) where some boxes are without a uncertainty flag. Our analysis show that nearly all inspected tracks ( $> 99\%$ ) are accurate, indicating the high-quality of amodal tracking annotations in TAO-amodal.

### 3.1. Statistical Analysis

We compare the statistics of TAO-Amodal to other amodal benchmarks in Table 1. For NuScenes, which only categorizes object visibilities into four buckets, we use interpolation to estimate the number of boxes below visibility 0.1 and 0.8. A few amodal datasets are omitted from the table either because they have been incorporated in TAO-Amodal [7, 61] or because these datasets lack quantified visibilities for categorizing distinct occlusion scenarios [9, 51]. TAO-Amodal encompasses annotations across an extensive 880 categories, which can be used to learn and evaluate object priors in a large-vocabulary setting, in contrast to benchmarks that only cover people or vehicles. Additionally, TAO-Amodal features a  $10\times$  longer evaluation duration, ensuring its status as a challenging benchmark.

## 4. Amodal tracking

**Traditional and amodal tracking.** Given a sequence of images  $I^1, I^2, \dots, I^t$ , tracking approaches aims to output modal bounding boxes  $b$ , trajectory identifiers  $\tau$ , and class labels  $s$  for objects across all frames. If an object is partially occluded, the box marks only the visible extent of the object, as illustrated in Fig. 2. We focus here on amodal trackers, which similarly takes as input a sequence of images,

| Method                  | Detection Metrics     |                         |                       |                   |              |              | Tracking Metrics |                       |              |
|-------------------------|-----------------------|-------------------------|-----------------------|-------------------|--------------|--------------|------------------|-----------------------|--------------|
|                         | AP <sup>[0,0.1]</sup> | AP <sup>[0.1,0.8]</sup> | AP <sup>[0.8,1]</sup> | AP <sup>OoF</sup> | Modal AP     | AP           | AP               | AP <sup>[0,0.8]</sup> | Modal AP     |
| QDTrack [17]            | 0.39                  | 7.79                    | 21.70                 | 7.88              | 20.07        | 15.47        | 7.84             | 4.03                  | 11.36        |
| TET [36]                | 0.70                  | 8.89                    | 29.96                 | 8.66              | 29.42        | 22.04        | 4.72             | 3.32                  | 7.7          |
| AOA [12]                | 0.56                  | 6.32                    | 24.14                 | 6.53              | 23.27        | 17.76        | 13.63            | 6.63                  | 21.18        |
| ViTDet-B + SORT [4, 37] | 0.77                  | 11.40                   | 34.03                 | 12.98             | 32.67        | 25.15        | 6.95             | 4.10                  | 11.57        |
| ViTDet-L + SORT [4, 37] | <b>1.18</b>           | 13.75                   | 37.41                 | 14.70             | 36.65        | 28.05        | 8.19             | 5.14                  | 13.73        |
| ViTDet-H + SORT [4, 37] | 1.03                  | <b>14.54</b>            | <b>39.71</b>          | <b>16.53</b>      | <b>38.05</b> | <b>29.56</b> | 8.94             | 5.76                  | 14.55        |
| GTR [64]                | 0.78                  | 13.24                   | 37.54                 | 14.18             | 36.08        | 28.19        | <b>16.02</b>     | <b>8.86</b>           | <b>22.50</b> |

Table 2. **Off-the-shelf trackers on TAO-Amodal validation set.** We use the metrics defined in Sec. 5.1, where the visibility range is indicated by the superscript. Off-the-shelf trackers were either trained on TAO [10] or on synthetic videos [64] generated using LVIS images [21], with categories aligned with our dataset. We use visibility attributes to analyze performance at various levels of occlusion. While certain trackers can detect non-occluded objects well (over 35% AP), objects that are highly occluded, partially occluded, and out-of-frame remain challenging. Because of GTR’s overall strong performance in both detection and tracking, we use it as the basis for our subsequent experiments. We run all existing trackers at 1 fps and average AP across all categories with an IoU threshold of 0.5.

| Method                                       | Detection Metrics     |                         |                       |                      |                      | Tracking Metrics     |                       |
|--|-----------------------|-------------------------|-----------------------|----------------------|----------------------|----------------------|-----------------------|
|  | AP <sup>[0,0.1]</sup> | AP <sup>[0.1,0.8]</sup> | AP <sup>[0.8,1]</sup> | AP <sup>OoF</sup>    | AP                   | AP                   | AP <sup>[0,0.8]</sup> |
| Baseline (GTR [64])                          | 0.78                  | 13.24                   | 37.54                 | 14.18                | 28.19                | 16.02                | 8.86                  |
| Fine-tune entire model                       | 0.52                  | 10.36                   | 24.08                 | 10.34                | 17.93                | 7.70                 | 3.93                  |
| Fine-tune regression head + proposal network | 0.79                  | 10.57                   | 27.91                 | 11.37                | 21.42                | 9.04                 | 4.53                  |
| Fine-tune regression head                    | 0.77                  | 14.62                   | 38.17                 | 15.31                | 29.24                | 16.07                | 9.28                  |
| Amodal Expander                              | 0.67                  | 16.29                   | 37.11                 | 17.39                | 29.50                | 16.10                | <b>10.44</b> (+1.58)  |
| Amodal Expander + PnO                        | <b>0.80</b> (+0.02)   | 16.41                   | 37.74                 | 17.64                | 29.87                | <b>16.35</b> (+0.33) | 10.13                 |
| Amodal Expander + PnO <sup>†</sup>           | 0.77                  | <b>16.53</b> (+3.29)    | <b>37.80</b> (+0.26)  | <b>17.65</b> (+3.47) | <b>29.96</b> (+1.77) | <b>16.35</b> (+0.33) | 10.28 (+1.42)         |

Table 3. **Amodal expander on TAO-Amodal validation set.** We ablate different strategies for repurposing GTR for amodal tracking, including fine-tuning all or part of the model, as well as our proposed Amodal Expander. The latter modestly outperforms naive fine-tuning of the regression head. When combined with additional augmentation techniques for generating synthetic occlusions such as PasteNOcclude (PnO) (as detailed in Sec 4.2), our final model produces noticeable gains for partially occluded and out-of-frame objects. All models (other than the baseline) were trained on TAO-Amodal training set for 20k iterations, while <sup>†</sup> denotes 45k iterations of training. Table 4 focuses on performance for the people category, demonstrating even more impressive gains.

output modal boxes  $b$ , trajectory identifiers  $\tau$ , and classes  $s$ . Beyond this, amodal tracker further generates amodal boxes  $b_a$ , which cover full extent of partially and fully occluded objects.

In reality, training an entire amodal model is unfeasible due to the limited amount of amodal training data. Drawing inspiration from the human ability of amodal completion, we posit the feasibility of transforming a conventional tracker into an amodal one by leveraging its understanding of modal objects. We introduced a light-weight class-agnostic amodal expander  $E$  in the next section.

#### 4.1. Amodal expander

Amodal expander  $E$  serves as a plug-in module to direct conventional trackers towards achieving amodal perception. For each object, amodal expander takes as input the modal box  $b$  and features  $f$ , which can be retrieved from the

tracker, and generates the amodal bounding boxes  $b_a$ .

**Predicting amodal boxes in a residual manner.** In practice, the amodal expander is crafted in a residual manner, akin to the structure in two-stage detectors [23, 46] and trackers [64]. As illustrated in Fig. 3, the tracker initially produces region proposal features  $f$  and modal proposals  $b$ , and subsequently refines  $b$  through a regression head  $R$  by predicting a modal box delta  $\Delta b$ . Our amodal expander receives modal box delta  $\Delta b$  and object feature  $f$  as input, generating amodal box delta. This delta is then applied to the modal proposal  $b$  to generate amodal boxes  $b_a$ , denoted as  $E(\Delta b, f) + b \approx b_a$ . The training of the amodal expander basically follows the training of regression head [46] by matching box proposals with a ground truth and applying regression loss. We first match modal box predictions  $b$  to a **modal** ground truth  $b^*$ . Then, we apply the regression loss,

| Method                             | Detection Metrics     |                         |                       |                       |                       | Tracking Metrics     |                       |
|------------------------------------|-----------------------|-------------------------|-----------------------|-----------------------|-----------------------|----------------------|-----------------------|
|                                    | AP <sup>[0,0.1]</sup> | AP <sup>[0.1,0.8]</sup> | AP <sup>[0.8,1]</sup> | AP <sup>OoF</sup>     | Overall               | Overall              | AP <sup>[0,0.8]</sup> |
| GTR [64]                           | 0.29                  | 37.15                   | 71.49                 | 42.07                 | 53.81                 | 17.47                | 14.39                 |
| FT regression head                 | 0.41                  | 49.32                   | 78.93                 | 53.26                 | 61.36                 | 20.44                | 18.74                 |
| Amodal Expander                    | 2.26                  | 71.64                   | 84.07                 | 73.74                 | 74.22                 | <b>26.77 (+9.30)</b> | 28.94                 |
| Amodal Expander <sup>†</sup>       | <b>2.46 (+2.17)</b>   | <b>71.86 (+34.71)</b>   | <b>84.21 (+12.72)</b> | <b>73.96 (+31.89)</b> | <b>74.34 (+20.53)</b> | 26.72                | <b>28.95 (+14.56)</b> |
| Amodal Expander + PnO              | 1.94                  | 69.87                   | 83.86                 | 72.58                 | 73.20                 | 26.68                | 28.76                 |
| Amodal Expander + PnO <sup>†</sup> | 1.99                  | 70.23                   | 84.00                 | 72.85                 | 73.38                 | 26.61                | 28.64                 |

Table 4. **Evaluating People on TAO-Amodal validation set.** We follow the conventions of Table 3 but evaluate performance only on the people category. Here, our Amodal Expander improves over the baseline by **more than 30% AP** for partially occluded and out-of-frame people. This notable improvement could also be observed in the qualitative results in Figure 5. Training without PasteNOcclude (PnO) yields a slight performance drop. We posit that this dramatic performance increase comes from the fact that people is the most common category. Our results suggest that adding synthetic (occluded) examples is more helpful for less common categories.

selected as smooth L1 [19], with the corresponding amodal ground truth  $b_a^*$ :

$$L(b, \Delta b, f) = L_{reg}(E(\Delta b, f) + b, b_a^*) \quad (1)$$

As later shown in Table 5, the matching strategy is crucial in the training of the expander. Amodal expander architecture is introduced in Sec. 5.2. The effectiveness of amodal expander is demonstrated in Tabs. 3 and 4.

#### 4.2. Crafting occlusion with PasteNOcclude (PnO)

To simulate occlusion scenarios during training, we introduced a data augmentation technique called PasteNOcclude (PnO). PasteNOcclude functions by integrating segments of objects into the original images to act as occludees. The segment collection comprises 505k objects extracted from LVIS [21] and COCO [38] images using segmentation masks. For each input image, we randomly select 1 to 7 segments from the collection and paste them at arbitrary locations, allowing for partial extension beyond the image boundary to replicate out-of-frame situations. Subsequently, we incorporate the ground truth boxes of the pasted segments into the original ground truth sets and apply regression loss according to the previously described pipeline. We find that PnO leads to improvements in detection across all occlusion scenarios, shown in Table 3. We posit that this synthetic strategy is particularly important for the long-tailed nature of TAO-amodal, unlike COCO-amodal, where a similar synthetic occlusion strategy leads to limited improvement [65]. We provide visual examples of such synthetic occlusions in the appendix.

### 5. Empirical analysis

Our experiments are categorized into two parts. In Section 5.1, we assess the challenges of amodal detection and tracking by evaluating various off-the-shelf trackers. The efficacy of the amodal expander is examined in Section 5.2. Implementation details and ablation study could be found in the appendix.

| Matching | Detection AP            |                   |              | Tracking AP  |                         |
|----------|-------------------------|-------------------|--------------|--------------|-------------------------|
|          | AP <sup>[0.1,0.8]</sup> | AP <sup>OoF</sup> | AP           | AP           | AP <sup>[0,1,0.8]</sup> |
| Modal    | 13.96                   | 14.92             | 28.64        | <b>16.45</b> | 8.96                    |
| Amodal   | <b>16.41</b>            | <b>17.64</b>      | <b>29.87</b> | 16.35        | <b>10.13</b>            |

Table 5. **Ablation: Region proposal matching strategy.** Given that existing off-the-shelf trackers generate modal proposals, direct matching with amodal ground truth yields suboptimal results. Our observation indicates that an improved strategy involves pairing region proposals with modal ground truth while applying regression loss to amodal predictions against the amodal ground truth. Both models are trained with PasteNOcclude (PnO) on TAO-Amodal training set for 20k iterations.

### 5.1. Benchmarking state-of-the-art trackers

**Evaluation Metrics.** Using the estimated visibility attributes, we assess the tracking and detection capabilities of the model through variations of detection AP [38] and Track-AP [10], representing the average precision across all categories at an IoU threshold of 0.5. We label objects with visibility less than 0.1 as heavily occluded, evaluated as AP<sup>[0.0, 0.1]</sup>, where the superscript indicates the range of object visibility. If the visibility falls between 0.1 and 0.8, we categorize them as partially occluded, while those with visibility greater than 0.8 are considered non-occluded. Objects that stretch partially beyond the image boundary are referred to as out-of-frame (OoF) and evaluated with AP<sup>OoF</sup>. Additionally, we assess the model’s performance on modal annotations with Modal AP. In tracking, we evaluate highly or partially occluded tracks (Track-AP<sup>[0, 0.8]</sup>), which are track with visibility at or below 0.8 for more than 5 frames (seconds). We also evaluate performance on modal annotations (Modal Track AP). A table is provided for easy reference to each metric definition in the appendix.

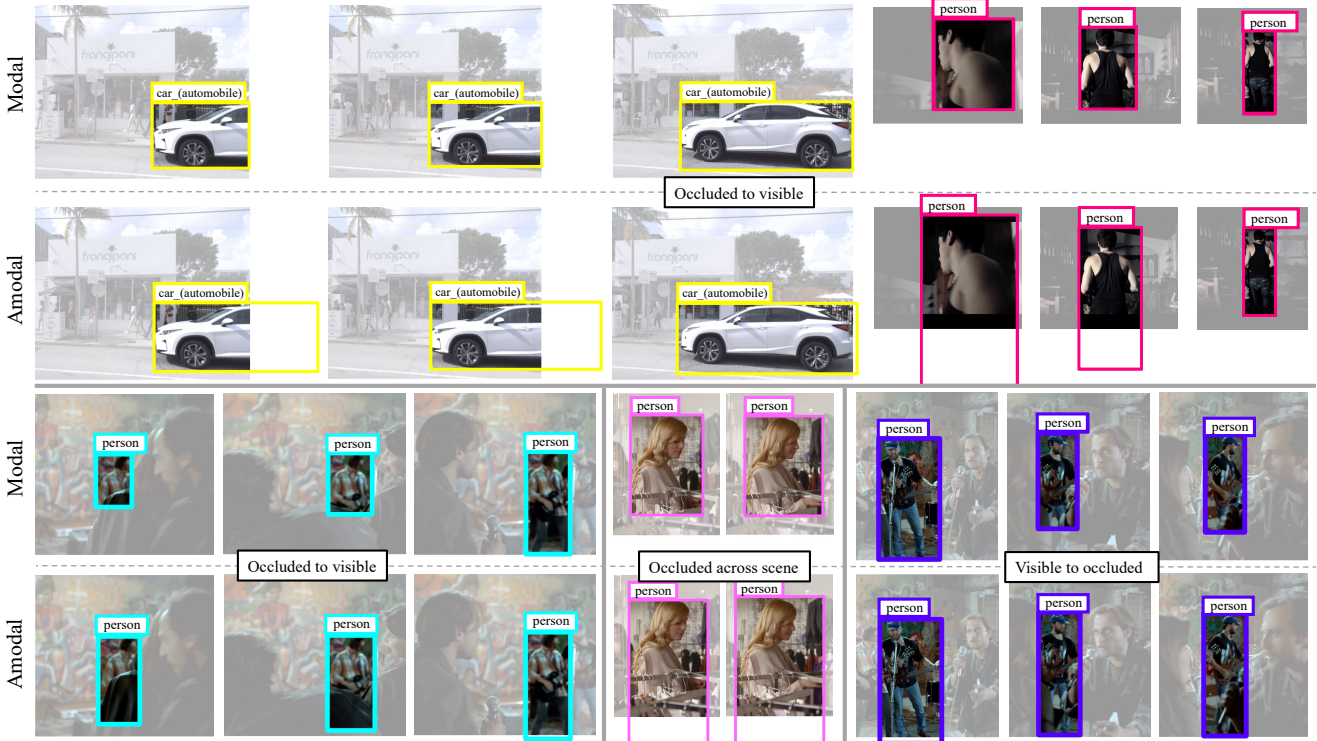


Figure 5. **Qualitative results of Amodal Expander on TAO-Amodal val.** Trackers augmented with our Amodal Expander produce predictions for both modal and amodal bounding boxes. In general, we are able to amodally complete objects that are occluded by objects in the scene (bottom-left) or objects that lie partially out of frame. Because we make use of online trackers that rely only on past evidence, we verify that our module can amodally complete objects that were occluded in the past as well as objects that become occluded later.

**Evaluation on TAO-Amodal validation set.** We report detection and tracking average precision (AP) numbers of SOTA off-the-shelf trackers on TAO-Amodal validation set running at 1fps with an IoU threshold 0.5 in Tab. 2. We also observed similar performance trends when running at 5fps with higher IoU thresholds, shown in the appendix. Every off-the-shelf tracker was trained on either TAO [10] or LVIS [21], ensuring alignment of category vocabulary with our dataset. GTR [64] was trained on the combination of LVIS and COCO [38] by generating synthetic videos using the training strategy in [63]. ViTDet [37] was trained on LVIS and combined with online SORT [4] tracker. We reproduced AOA [12] using their released implementation, with object detector trained on LVIS and tracking ReID head trained on TAO. QDTrack [17] and TET [36] followed similar training procedures, pretraining detectors on LVIS and training instance similarity heads on TAO.

**How well do standard trackers generalize to amodal perception?** Table 2 reveals notable differences in detection AP between modal (Modal AP) and amodal annotations (AP), amounting to an 8.49% difference. Additionally, the amodal tracking AP experiences a substantial decline

compared to modal tracking AP. These findings confirm our expectation that existing trackers struggle to generalize effectively to amodal perception.

**How well do standard trackers handle occlusion?** Existing off-the-shelf trackers exhibit reasonable performance in detecting non-occluded objects, with ViTDet achieving 39.71% AP<sup>[0.8,1]</sup> as revealed in Table 2. However, all trackers face challenges in detecting heavily occluded objects, and there is a noticeable decline in performance in partially occluded (AP<sup>[0.1,0.8]</sup>) and out-of-frame (OoF) scenarios. We noticed that ViTDet operating at 5 fps benefits from the property of SORT to estimate the location in the current frame using past information, resulting in improved results shown in the appendix. Nevertheless, this improvement comes at the cost of processing ViTDet on 5x more frames than models running at 1 fps. In contrast, amodal completion could be a promising way for efficiently handling occlusion.

## 5.2. Amodal expander experiments

Amodal expander architecture could be referred in Fig. 4. We built the expander on top of GTR [64] as this method



Figure 6. **Qualitative results of Amodal Expander across diverse categories on TAO-Amodal val.** Though we achieve the most impressive results for people, our Amodal Expander is effective across a diverse set of categories.

shows reasonable performance in both detection and tracking aspects in Table 2. The hidden dimension of MLP is selected as 256. ReLU [1] and dropout [48] with a probability of 0.2 were applied to each layer except the last one. The training of the amodal expander was conducted on the TAO-Amodal training set, along with PasteNOcclude (PnO) and augmentation used in [64]. All the modules except the amodal expander are frozen during training. Other ablation study, hyperparameter details for training and PnO could be found in the appendix.

**Amodal expander or fine-tuning?** We evaluated amodal expander on TAO-Amodal validation set as shown in Tab. 3. Amodal expander trained with PnO for 45k iterations achieved 3.29% and 3.47% performance win under partially occluded ( $AP^{[0.1, 0.8]}$ ) and out-of-frame ( $AP^{OOF}$ ) scenario. We also experimented with different fine-tuning strategies. Fine-tuning entire model or solely the regression head and proposal network resulted in performance degradation. We posit that, with only 500 amodal training sequences, the models struggle to completely *discard* modal knowledge. Fine-tuning box regression head is suboptimal when compared to amodal expander. Amodal expander further provides flexibility to adjust the architecture and select different input information, which are both important as later shown in the ablation section.

**Detecting people with amodal expander.** In Table 4, we study how well amodal expander detects and tracks people, which serves as a crucial category in many autonomous driving and tracking benchmarks. Amodal expander obtains a near 2x dramatic improvement compared to the baseline, with over 30% gain on  $AP^{[0.1, 0.8]}$  and  $AP^{OOF}$ . Tracking on highly or partially occluded people (Track- $AP^{[0.0, 0.8]}$ ) are also increased by 14.56%. This shows that one can obtain a strong amodal people tracker that could also track objects of diverse category vocabulary with our dataset.

**Proposal matching strategy matters.** To apply regression loss, training a box prediction head requires matching each region proposal to a ground truth box. A naive strategy is to directly match the region proposals to the amodal ground truth box. Nevertheless, as shown in Table 5, direct matching with amodal boxes leads to suboptimal results. We noted that since standard trackers generate modal region proposals, the model faced challenges in aligning proposals with the accurate ground truth due to a low Intersection over Union (IoU) between modal proposals and amodal ground truth. Consequently, we opted to match region proposals with modal bounding boxes and applied regression losses using amodal ground truth boxes.

## 6. Discussion

In this work, we focus on amodal perception of real-world objects. We draw inspiration from cognitive functions of amodal completion and object permanence in humans, that develop at an early age. Despite this, advancements in perception stacks like object detection and tracking, do not make amodal understanding central. We bring focus to three aspects/stages of building amodal perception stacks. First, we contribute a benchmark that annotates 880 categories of objects amodally in unconstrained indoor and outdoor settings, under partial and complete occlusion. Second, we contribute a benchmarking protocol in the form of metrics that evaluate detection and tracking specifically for the cases of partial or complete occlusions. Our key finding here is that existing algorithms fail dramatically on these metrics. To recover from this lack of performance on amodal detection and tracking and as a third contribution, we propose a light-weight and easy to train module, which we term as the Amodal Expander. Given modal boxes of objects, the expander learns to amodally complete the object bounding boxes till the extent of their occlusion. This simple fix gives us a boost of upto  $\sim 30$  AP points, specifically on the case of people.

## Appendix

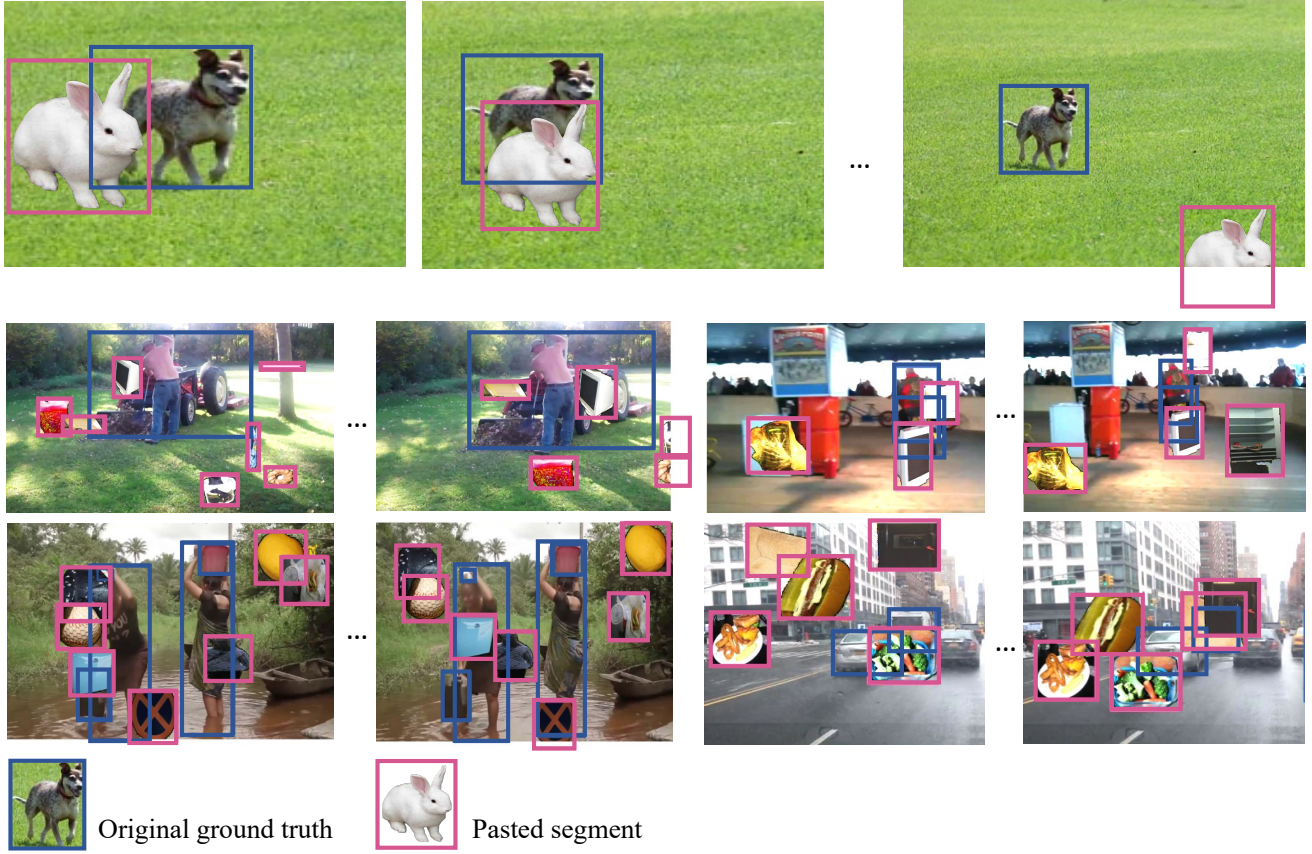


Figure 7. **Synthetic occlusions with PasteNOcclude (PnO).** PnO allows us to manually simulate occlusion scenarios and out-of-frame scenarios. We randomly choose 1 to 7 segments from a collection sourced from LVIS [21] and COCO [38] for pasting. For each inserted segment, we randomly determine the object’s size and position in the first and last frames. The size and location of the segment in intermediate frames are then generated through linear interpolation.

In this appendix, we extend our discussion of the proposed dataset and method within the context of tracking any object with amodal perception. Specifically, we discuss details about the training and PasteNOcclude technique in Section 7, provide further empirical analysis in Section 8, and outline the annotation guidelines of our dataset in Section 9. We further provide comprehensive video demonstration of our dataset and qualitative results at <https://tao-amodal.github.io>.

## 7. Implementation details

**Training Amodal Expander.** We trained amodal expander on TAO-Amodal training set for 20k iterations for all experiments unless specified. We used a 2-layer MLP as the architecture. The hidden dimension of MLP is selected as 256. ReLU [1] and dropout [48] with a probability of 0.2 were applied to each layer except the last one. Note

that amodal expander is compatible with any existing detector or tracker. However, in our experiments, we implemented the expander in conjunction with GTR [64]. Additional architecture details of GTR align with the selection in [64]. We used 0.01 as the base learning rate and applied WarmupCosineLR [24] as the scheduler. The optimizer is selected as AdamW [40]. The batch size for training is 4. We adopted the training methodology outlined in [64], treating each image as an independent sequence. Data augmentation [63], which includes random cropping and resizing, was applied to each image to produce synthetic videos with a length of 8 frames. Beyond this, we further applied PasteNOcclude, introduced in Sec. 4.2 in the main paper, on top of the synthetic videos to automatically generate more occlusion scenarios. We provide the hyperparameter details of PasteNOcclude in the next section.

| Method                  | Detection AP <sub>0.5:0.95</sub> |                         |                       |                   |              |              | Tracking AP <sub>0.5:0.95</sub> |                       |
|-------------------------|----------------------------------|-------------------------|-----------------------|-------------------|--------------|--------------|---------------------------------|-----------------------|
|                         | AP <sup>[0,0.1]</sup>            | AP <sup>[0.1,0.8]</sup> | AP <sup>[0.8,1]</sup> | AP <sup>OoF</sup> | Modal AP     | AP           | AP                              | AP <sup>[0,0.8]</sup> |
| QDTrack [17]            | 0.12                             | 2.29                    | 13.03                 | 2.90              | 12.64        | 8.53         | 3.36                            | 1.52                  |
| TET [36]                | 0.21                             | 2.71                    | 17.27                 | 3.14              | 17.58        | 11.80        | 1.99                            | 1.14                  |
| AOA [12]                | 0.26                             | 1.87                    | 15.98                 | 2.84              | 16.36        | 10.52        | 6.59                            | 2.07                  |
| ViTDet-B + SORT [4, 37] | 0.33                             | 3.41                    | 19.67                 | 5.02              | 19.83        | 13.39        | 3.03                            | 1.40                  |
| ViTDet-L + SORT [4, 37] | <b>0.43</b>                      | 4.14                    | 22.08                 | 5.81              | 22.65        | 15.35        | 4.16                            | 1.84                  |
| ViTDet-H + SORT [4, 37] | 0.36                             | 4.38                    | 23.62                 | <b>6.67</b>       | 23.89        | 16.21        | 4.24                            | 1.94                  |
| GTR [64]                | 0.24                             | <b>4.60</b>             | <b>26.01</b>          | 6.62              | <b>26.83</b> | <b>18.07</b> | <b>7.52</b>                     | <b>3.05</b>           |

Table 6. **Off-the-shelf trackers on TAO-Amodal validation with higher IoU thresholds.** The definitions of our evaluation metrics can be found in Table 10. The AP numbers are averaged over 10 IoU values from 0.5 to 0.95 with a 0.05 step, denoted as AP<sub>0.5 : 0.95</sub>. We observed a similar performance trend as results evaluated with an IoU threshold 0.5. We run all trackers at 1 fps.

| Method                  | Detection AP          |                         |                       |                   |              |              | Tracking AP  |                       |              |
|-------------------------|-----------------------|-------------------------|-----------------------|-------------------|--------------|--------------|--------------|-----------------------|--------------|
|                         | AP <sup>[0,0.1]</sup> | AP <sup>[0.1,0.8]</sup> | AP <sup>[0.8,1]</sup> | AP <sup>OoF</sup> | Modal AP     | AP           | AP           | AP <sup>[0,0.8]</sup> | Modal AP     |
| QDTrack [17]            | 0.42                  | 7.59                    | 21.53                 | 7.78              | 19.98        | 15.42        | 6.63         | 2.72                  | 10.34        |
| TET [36]                | 0.24                  | 5.39                    | 14.56                 | 4.73              | 29.42        | 10.51        | 3.52         | 2.21                  | 5.56         |
| AOA [12]                | 0.56                  | 6.29                    | 24.35                 | 6.77              | 23.51        | 17.85        | 12.82        | 5.53                  | 20.67        |
| ViTDet-B + SORT [4, 37] | 1.00                  | 13.38                   | 37.98                 | 14.78             | 37.08        | 28.32        | 10.09        | 4.40                  | 16.93        |
| ViTDet-L + SORT [4, 37] | <b>1.32</b>           | 16.38                   | 43.30                 | 17.16             | 42.31        | 32.08        | 11.75        | 5.53                  | 19.22        |
| ViTDet-H + SORT [4, 37] | 1.06                  | <b>17.24</b>            | <b>45.18</b>          | <b>18.58</b>      | <b>44.02</b> | <b>33.53</b> | 13.16        | 5.87                  | <b>21.39</b> |
| GTR [64]                | 0.57                  | 12.45                   | 35.89                 | 13.63             | 34.92        | 27.28        | <b>13.70</b> | <b>7.02</b>           | 20.09        |

Table 7. **Off-the-shelf trackers on TAO-Amodal validation set running at 5 fps.** In contrast to results shown in Table 2 in the main paper, ViTDet [37] with SORT [4] achieves a performance gain by running at a higher fps as SORT [4] leverages its capability to estimate the location in the current frame based on the location in previous frames. AP numbers are averaged across all categories at an IoU threshold 0.5.

| Method             | Detection AP            |                   |              | Tracking AP  |                       |
|--------------------|-------------------------|-------------------|--------------|--------------|-----------------------|
|                    | AP <sup>[0,1,0.8]</sup> | AP <sup>OoF</sup> | AP           | AP           | AP <sup>[0,0.8]</sup> |
| $\Delta b$         | 13.86                   | 14.79             | 28.62        | <b>16.47</b> | 8.94                  |
| $f$                | 16.12                   | 17.08             | 29.58        | 16.12        | 10.08                 |
| $f$ and $\Delta b$ | <b>16.41</b>            | <b>17.64</b>      | <b>29.87</b> | 16.35        | <b>10.13</b>          |

Table 8. **Input to Amodal Expander.** Modal box (deltas)  $\Delta b$ , output by the regression head as shown in Fig. 3 in the main paper, contains information about the exact location of modal box predictions. Object features  $f$  encompass the visual appearance information of the modal proposals. We found that both information are important in amodally inferring the object’s shape. All models were trained on TAO-Amodal training set with PasteNOclude (PnO) for 20k iterations.

**PasteNOclude (PnO).** The visual example of PnO is illustrated in Fig. 7. To collect the segments as occluders from LVIS [21] and COCO [38], we utilize segmentation mask to mask out the background area and employ the

| # layers | Detection AP            |                   |              | Tracking AP  |                       |
|----------|-------------------------|-------------------|--------------|--------------|-----------------------|
|          | AP <sup>[0,1,0.8]</sup> | AP <sup>OoF</sup> | AP           | AP           | AP <sup>[0,0.8]</sup> |
| 1-layer  | 13.78                   | 15.19             | 28.21        | 14.29        | 8.12                  |
| 2-layer  | <b>16.41</b>            | <b>17.64</b>      | <b>29.87</b> | <b>16.35</b> | <b>10.13</b>          |
| 4-layer  | 15.55                   | 17.02             | 29.41        | 16.35        | 9.99                  |
| 6-layer  | 14.55                   | 15.64             | 28.79        | 16.05        | 9.09                  |

Table 9. **Number of MLP layers in Amodal Expander.** Empirically, using a lightweight 2-layer MLP amodal expander proves sufficient to generate reasonable amodal detection results. All models were trained on TAO-Amodal training set for 20k iterations.

bounding box to crop the object. We filter out those segments where the mask area is less than 70% of the bounding box area to ensure the object (occluder) is not occluded. In the training process, we view each image as a sequence and create an 8-frame sequence employing the data augmentation strategy outlined in [64] based on each single image.

| Metric                 | Definition  | Type              |
|------------------------|---|-------------------|
| AP                     | Average Precision (AP) averaged across all categories at an IoU threshold 0.5.                              |                   |
| $AP^{[0, 0.1]}$        | AP for heavily occluded objects, with visibility smaller than 0.1.  |                   |
| $AP^{[0.1, 0.8]}$      | AP for partially occluded objects, with visibility in $[0.1, 0.8]$ .  |                   |
| $AP^{[0.8, 1.0]}$      | AP for non-occluded objects, with visibility larger than 0.8.   | Detection Metrics |
| $AP^{OoF}$             | AP for partially out-of-frame (OoF) objects.  |                   |
| Modal AP               | AP on modal annotations.  |                   |
| Track-AP [10]          | Average Precision of a track averaged across all categories at an 3D IoU threshold 0.5.                     |                   |
| Track-AP $^{[0, 0.8]}$ | Track-AP for any track that is occluded, with visibility at or below 0.8, for more than 5 frames (seconds). | Tracking Metrics  |
| Modal Track-AP         | Track-AP on modal annotations   |                   |

Table 10. **Evaluation metrics with IoU threshold 0.5.** We define variations of AP [38] and Track-AP [10] based on levels of occlusion.

| Occlusion type   | Extent   | Cases   | Instructions  |
|------------------|----------|---|---|
| In-frame         | Partial  | Partially occluded before being fully visible | Annotate with best estimate using category label  |
|                  |          | Partially occluded after being fully visible  | Annotate with best estimate   |
|                  | Complete | Invisible before being (partially) visible    | Only annotate if the object has been visible before   |
|                  |          | Invisible after being (partially) visible     | If confident, annotate with best estimate<br>If not, only annotate till the last visible frame  |
|                  |          | Invisible for a while                         | If confident, annotate with best estimate<br>If not, still annotate but add an uncertainty flag |
| Out-of-frame     | Partial  | Object goes beyond image border               | Only annotate inside the annotation workspace   |
|                  |          | Object goes beyond the padded image           | Clip at the border of the padded image  |
|                  | Complete | -   | -   |
| Behind-the-frame | Partial  | Object is in front of and behind the camera   | Only label the part of object in front of camera  |
|                  | Complete | -   | -   |

Table 11. **Annotation guidelines.** TAO-Amodal is annotated with the guidelines above, which taxonomizes occlusions across severity (partial versus complete) and type (in/out-of-frame). As mentioned in Sec. 3 in the main paper, we scope out the case where an object may be present behind the camera. For out-of-frame occlusions, we limit the *annotation workspace* to be twice the image size.

Subsequently, we randomly select 1 to 7 segments from the collection and place them at random locations. Additionally, we randomly adjust the height and width of the inserted segments within the range of [12, 192]. To maintain smooth transitions between consecutive frames, we randomly determine the object’s location and size only in the first and last frames. The size and location in intermediate frames are obtained through interpolation.

## 8. More empirical analysis

We used the same evaluation metrics defined in Section 5.1 in the main paper. For easy reference, we summarize all the definitions in Table 10. We presented additional experiments involving state-of-the-art trackers in Section 8.1 and the amodal expander in Section 8.2.

### 8.1. Benchmarking off-the-shelf-trackers

**Evaluation with higher IoU thresholds.** In Table 6, we evaluate the trackers with average precision (AP) averaged over 10 IoU thresholds from 0.5 to 0.95 at a step 0.05. The performance trend basically aligns with what we observed in Table 2 in the main paper. GTR [64] obtained strong performance in both detection and tracking. When evaluated with higher IoU thresholds, ViTDet [37] and SORT [4] demonstrate inferior detection performance compared to GTR, indicating a contrasting outcome compared to the results obtained at a 0.5 threshold. This shows the limitations of SORT [4] in accurately estimating bounding boxes.

**Running trackers at higher fps.** We reported the performance of state-of-the-art trackers running at 5 fps in Tab. 7. We noticed that ViTDet [37] along with SORT [4] achieved the best performance among all the trackers. This aligns with our intuition as SORT estimates the location in the current frame based on prior-frame locations. This property benefits from running at higher fps. Nevertheless, achieving this performance improvement requires processing ViTDet on five times more frames than models operating at 1 fps, leading to increased computational demands.

## 8.2. Amodal expander experiments

**Investigating key information for amodal box inference.** Table 8 reports different input choices to the amodal expander. Modal box (deltas)  $\Delta b$ , output by the regression head as shown in Fig. 3 in the main paper, are used to yield final modal box predictions when applied to region proposals and thus contain information about the exact location of modal box predictions. Proposal features encompass visual appearance information of the detected region proposals. Absence of visual cues significantly diminishes the performance of both detection and tracking under occlusion. Interestingly, the amodal expander, incorporating both modal delta and proposal features, yielded the most favorable outcomes, indicating that, beyond visual information, estimating modal box locations also contributes to effective amodal reasoning.

**Number of MLP layers.** We tested with the depth of amodal expander architecture in Table 9. We observe a reverse-U pattern concerning the number of MLP layers, with two-layer MLPs demonstrating superior performance compared to other models. A one-layer MLP proves sub-optimal in both detection and tracking. Notably, using a 1-layer MLP results in slightly inferior outcomes compared to fine-tuning the regression head, as indicated in Table 3 in the main paper. Our contention is that the regression head may derive benefits from pre-training on modal benchmarks.

## 9. Annotation guidelines

We ensure high-quality annotations by requiring annotators to follow the guidelines detailed in Table 11. Our coverage spans various occlusion scenarios, encompassing in-frame, out-of-frame, or behind-the-scene situations, where an object may be partially obscured behind the camera.

## References

- [1] Abien Fred Agarap. Deep learning using rectified linear units (relu). *arXiv preprint arXiv:1803.08375*, 2018. 8, 9
- [2] Ali Athar, Jonathon Luiten, Paul Voigtlaender, Tarasha Khurana, Achal Dave, Bastian Leibe, and Deva Ramanan. Burst: A benchmark for unifying object recognition, segmentation and tracking in video. In *Proceedings of the IEEE/CVF Winter Conference on Applications of Computer Vision*, pages 1674–1683, 2023. 2, 3
- [3] Renée Baillargeon and Julie DeVos. Object permanence in young infants: Further evidence. *Child development*, 62(6): 1227–1246, 1991. 1
- [4] Alex Bewley, Zongyuan Ge, Lionel Ott, Fabio Ramos, and Ben Upcroft. Simple online and realtime tracking. In *2016 IEEE international conference on image processing (ICIP)*, pages 3464–3468. IEEE, 2016. 3, 5, 7, 10, 11, 12
- [5] Holger Caesar, Varun Bankiti, Alex H Lang, Sourabh Vora, Venice Erin Liang, Qiang Xu, Anush Krishnan, Yu Pan, Giancarlo Baldan, and Oscar Beijbom. nuscenes: A multimodal dataset for autonomous driving. *arXiv preprint arXiv:1903.11027*, 2019. 2, 3
- [6] Jiarui Cai, Mingze Xu, Wei Li, Yuanjun Xiong, Wei Xia, Zhiwen Tu, and Stefano Soatto. Memot: Multi-object tracking with memory. In *Proceedings of the IEEE/CVF Conference on Computer Vision and Pattern Recognition*, pages 8090–8100, 2022. 3
- [7] Ming-Fang Chang, John Lambert, Patsorn Sangkloy, Jagjeet Singh, Slawomir Bak, Andrew Hartnett, De Wang, Peter Carr, Simon Lucey, Deva Ramanan, et al. Argoverse: 3d tracking and forecasting with rich maps. In *Proceedings of the IEEE Conference on Computer Vision and Pattern Recognition*, pages 8748–8757, 2019. 2, 3, 4
- [8] Yuhua Chen, Wen Li, Christos Sakaridis, Dengxin Dai, and Luc Van Gool. Domain adaptive faster r-cnn for object detection in the wild. In *Proceedings of the IEEE conference on computer vision and pattern recognition*, pages 3339–3348, 2018. 3
- [9] Anthony Cioppa, Silvio Giancola, Adrien Deliege, Le Kang, Xin Zhou, Zhiyu Cheng, Bernard Ghanem, and Marc Van Droogenbroeck. Soccernet-tracking: Multiple object tracking dataset and benchmark in soccer videos. In *Proceedings of the IEEE/CVF Conference on Computer Vision and Pattern Recognition*, pages 3491–3502, 2022. 1, 4
- [10] Achal Dave, Tarasha Khurana, Pavel Tokmakov, Cordelia Schmid, and Deva Ramanan. Tao: A large-scale benchmark for tracking any object. In *Computer Vision–ECCV 2020: 16th European Conference, Glasgow, UK, August 23–28, 2020, Proceedings, Part V 16*, pages 436–454. Springer, 2020. 1, 2, 5, 6, 7, 11
- [11] Patrick Dendorfer, Hamid Rezatofighi, Anton Milan, Javen Shi, Daniel Cremers, Ian Reid, Stefan Roth, Konrad Schindler, and Laura Leal-Taixé. Mot20: A benchmark for multi object tracking in crowded scenes. *arXiv preprint arXiv:2003.09003*, 2020. 2, 3
- [12] Fei Du, Bo Xu, Jiasheng Tang, Yuqi Zhang, Fan Wang, and Hao Li. 1st place solution to eccv-tao-2020: Detect and represent any object for tracking. *arXiv preprint arXiv:2101.08040*, 2021. 1, 5, 7, 10
- [13] Yunhao Du, Zhicheng Zhao, Yang Song, Yanyun Zhao, Fei Su, Tao Gong, and Hongying Meng. Strongsort: Make deepsort great again. *IEEE Transactions on Multimedia*, 2023. 3
- [14] Kiana Ehsani, Roozbeh Mottaghi, and Ali Farhadi. Segan: Segmenting and generating the invisible. In *CVPR*, 2018. 3
- [15] Mark Everingham, Luc Van Gool, Christopher KI Williams, John Winn, and Andrew Zisserman. The pascal visual object classes (voc) challenge. *International journal of computer vision*, 88(2):303–338, 2010. 1
- [16] Heng Fan, Liting Lin, Fan Yang, Peng Chu, Ge Deng, Sijia Yu, Hexin Bai, Yong Xu, Chunyuan Liao, and Haibin Ling. Lasot: A high-quality benchmark for large-scale single object tracking. In *Proceedings of the IEEE/CVF conference on computer vision and pattern recognition*, pages 5374–5383, 2019. 1, 3
- [17] Tobias Fischer, Thomas E Huang, Jiangmiao Pang, Linlu Qiu, Haofeng Chen, Trevor Darrell, and Fisher Yu. Qdtrack: Quasi-dense similarity learning for appearance-only multiple object tracking. *IEEE Transactions on Pattern Analysis and Machine Intelligence*, 2023. 1, 5, 7, 10
- [18] Andreas Geiger, Philip Lenz, and Raquel Urtasun. Are we ready for autonomous driving? the kitti vision benchmark suite. In *CVPR*, pages 3354–3361. IEEE, 2012. 2
- [19] Ross Girshick. Fast r-cnn. In *Proceedings of the IEEE international conference on computer vision*, pages 1440–1448, 2015. 4, 6
- [20] Chunhui Gu, Chen Sun, David A Ross, Carl Vondrick, Caroline Pantofaru, Yeqing Li, Sudheendra Vijayanarasimhan, George Toderici, Susanna Ricco, Rahul Sukthankar, et al. Ava: A video dataset of spatio-temporally localized atomic visual actions. In *Proceedings of the IEEE conference on computer vision and pattern recognition*, pages 6047–6056, 2018. 3
- [21] Agrim Gupta, Piotr Dollar, and Ross Girshick. Lvis: A dataset for large vocabulary instance segmentation. In *Proceedings of the IEEE/CVF Conference on Computer Vision and Pattern Recognition*, pages 5356–5364, 2019. 1, 3, 5, 6, 7, 9, 10
- [22] Xiaotian Han, Quanzeng You, Chunyu Wang, Zhizheng Zhang, Peng Chu, Houdong Hu, Jiang Wang, and Zicheng Liu. Mmptrack: Large-scale densely annotated multi-camera multiple people tracking benchmark. In *Proceedings of the IEEE/CVF Winter Conference on Applications of Computer Vision*, pages 4860–4869, 2023. 2
- [23] Kaiming He, Georgia Gkioxari, Piotr Dollár, and Ross Girshick. Mask R-CNN. In *ICCV*, 2017. 5
- [24] Tong He, Zhi Zhang, Hang Zhang, Zhongyue Zhang, Junyuan Xie, and Mu Li. Bag of tricks for image classification with convolutional neural networks. In *Proceedings of the IEEE/CVF conference on computer vision and pattern recognition*, pages 558–567, 2019. 9
- [25] Cheng-Yen Hsieh, Chih-Jung Chang, Fu-En Yang, and Yu-Chiang Frank Wang. Self-supervised pyramid representation learning for multi-label visual analysis and beyond. In *Proceedings of the IEEE/CVF Winter Conference on Applications of Computer Vision*, pages 2696–2705, 2023. 1

- [26] Yuan-Ting Hu, Hong-Shuo Chen, Kexin Hui, Jia-Bin Huang, and Alexander G Schwing. Sail-vos: Semantic amodal instance level video object segmentation-a synthetic dataset and baselines. In *Proceedings of the IEEE/CVF Conference on Computer Vision and Pattern Recognition*, pages 3105–3115, 2019. 3
- [27] Yuan-Ting Hu, Jiahong Wang, Raymond A Yeh, and Alexander G Schwing. Sail-vos 3d: A synthetic dataset and baselines for object detection and 3d mesh reconstruction from video data. In *Proceedings of the IEEE/CVF Conference on Computer Vision and Pattern Recognition*, pages 1418–1428, 2021. 3
- [28] Michael Kavsek. The influence of context on amodal completion in 5-and 7-month-old infants. *Journal of Cognition and Development*, 5(2):159–184, 2004. 1
- [29] Mehran Khodabandeh, Arash Vahdat, Mani Ranjbar, and William G Macready. A robust learning approach to domain adaptive object detection. In *Proceedings of the IEEE/CVF International Conference on Computer Vision*, pages 480–490, 2019. 3
- [30] Tarasha Khurana, Achal Dave, and Deva Ramanan. Detecting invisible people. In *Proceedings of the IEEE/CVF International Conference on Computer Vision*, pages 3174–3184, 2021. 2, 3, 4
- [31] Ivan Krasin, Tom Duerig, Neil Alldrin, Vittorio Ferrari, Sami Abu-El-Haija, Alina Kuznetsova, Hassan Rom, Jasper Uijlings, Stefan Popov, Andreas Veit, Serge Belongie, Victor Gomes, Abhinav Gupta, Chen Sun, Gal Chechik, David Cai, Zheyun Feng, Dhyane Narayanan, and Kevin Murphy. Openimages: A public dataset for large-scale multi-label and multi-class image classification. *Dataset available from https://github.com/openimages*, 2017. 1, 3
- [32] Matej Kristan, Ales Leonardis, Jiri Matas, Michael Felsberg, Roman Pflugfelder, Luka Čehovin Zajc, Tomas Vojir, Goutam Bhat, Alan Lukezic, Abdelrahman Elde索key, et al. The sixth visual object tracking vot2018 challenge results. In *Proceedings of the European conference on computer vision (ECCV) workshops*, pages 0–0, 2018. 1
- [33] Laura Leal-Taixé, Anton Milan, Ian Reid, Stefan Roth, and Konrad Schindler. Motchallenge 2015: Towards a benchmark for multi-target tracking. *arXiv preprint arXiv:1504.01942*, 2015. 2
- [34] Feng Li, Hao Zhang, Huaizhe Xu, Shilong Liu, Lei Zhang, Lionel M Ni, and Heung-Yeung Shum. Mask dino: Towards a unified transformer-based framework for object detection and segmentation. In *Proceedings of the IEEE/CVF Conference on Computer Vision and Pattern Recognition*, pages 3041–3050, 2023. 1
- [35] Ke Li and Jitendra Malik. Amodal instance segmentation. In *ECCV*. Springer, 2016. 3
- [36] Siyuan Li, Martin Danelljan, Henghui Ding, Thomas E Huang, and Fisher Yu. Tracking every thing in the wild. In *European Conference on Computer Vision*, pages 498–515. Springer, 2022. 1, 5, 7, 10
- [37] Yanghao Li, Hanzi Mao, Ross Girshick, and Kaiming He. Exploring plain vision transformer backbones for object detection. In *European Conference on Computer Vision*, pages 280–296. Springer, 2022. 1, 5, 7, 10, 11, 12
- [38] Tsung-Yi Lin, Michael Maire, Serge Belongie, James Hays, Pietro Perona, Deva Ramanan, Piotr Dollár, and C Lawrence Zitnick. Microsoft coco: Common objects in context. In *European conference on computer vision*, pages 740–755. Springer, 2014. 1, 6, 7, 9, 10, 11
- [39] Huan Ling, David Acuna, Karsten Kreis, Seung Wook Kim, and Sanja Fidler. Variational amodal object completion. *Advances in Neural Information Processing Systems*, 33: 16246–16257, 2020. 3
- [40] Ilya Loshchilov and Frank Hutter. Decoupled weight decay regularization. *arXiv preprint arXiv:1711.05101*, 2017. 9
- [41] Tim Meinhart, Alexander Kirillov, Laura Leal-Taixé, and Christoph Feichtenhofer. Trackformer: Multi-object tracking with transformers. In *Proceedings of the IEEE/CVF conference on computer vision and pattern recognition*, pages 8844–8854, 2022. 1
- [42] Anton Milan, Laura Leal-Taixé, Ian Reid, Stefan Roth, and Konrad Schindler. Mot16: A benchmark for multi-object tracking. *arXiv preprint arXiv:1603.00831*, 2016. 2, 3
- [43] Yumiko Otsuka, So Kanazawa, and Masami K Yamaguchi. Development of modal and amodal completion in infants. *Perception*, 35(9):1251–1264, 2006. 1
- [44] Lu Qi, Li Jiang, Shu Liu, Xiaoyong Shen, and Jiaya Jia. Amodal instance segmentation with KINS dataset. In *CVPR*, 2019. 2, 3
- [45] N Dinesh Reddy, Minh Vo, and Srinivasa G Narasimhan. Carfusion: Combining point tracking and part detection for dynamic 3d reconstruction of vehicles. In *Proceedings of the IEEE conference on computer vision and pattern recognition*, pages 1906–1915, 2018. 2
- [46] Shaoqing Ren, Kaiming He, Ross Girshick, and Jian Sun. Faster r-cnn: Towards real-time object detection with region proposal networks. In *Advances in neural information processing systems*, pages 91–99, 2015. 1, 5
- [47] Gunnar A Sigurdsson, Gü̈l Varol, Xiaolong Wang, Ali Farhadi, Ivan Laptev, and Abhinav Gupta. Hollywood in homes: Crowdsourcing data collection for activity understanding. In *Computer Vision–ECCV 2016: 14th European Conference, Amsterdam, The Netherlands, October 11–14, 2016, Proceedings, Part I 14*, pages 510–526. Springer, 2016. 3
- [48] Nitish Srivastava, Geoffrey Hinton, Alex Krizhevsky, Ilya Sutskever, and Ruslan Salakhutdinov. Dropout: a simple way to prevent neural networks from overfitting. *The journal of machine learning research*, 15(1):1929–1958, 2014. 8, 9
- [49] Colton Stearns, Davis Rempe, Jie Li, Rareş Ambruş, Sergey Zakharov, Vitor Guizilini, Yanchao Yang, and Leonidas J Guibas. Spot: Spatiotemporal modeling for 3d object tracking. In *European Conference on Computer Vision*, pages 639–656. Springer, 2022. 3
- [50] Pei Sun, Henrik Kretzschmar, Xerxes Dotiwalla, Aurelien Chouard, Vijaysai Patnaik, Paul Tsui, James Guo, Yin Zhou, Yuning Chai, Benjamin Caine, et al. Scalability in perception for autonomous driving: Waymo open dataset. In *Proceedings of the IEEE/CVF Conference on Computer Vision and Pattern Recognition*, pages 2446–2454, 2020. 2

- [51] Peize Sun, Jinkun Cao, Yi Jiang, Zehuan Yuan, Song Bai, Kris Kitani, and Ping Luo. Dancetrack: Multi-object tracking in uniform appearance and diverse motion. In *Proceedings of the IEEE/CVF Conference on Computer Vision and Pattern Recognition*, pages 20993–21002, 2022. 4
- [52] Bart Thomee, David A Shamma, Gerald Friedland, Benjamin Elizalde, Karl Ni, Douglas Poland, Damian Borth, and Li-Jia Li. Yfcc100m: The new data in multimedia research. *Communications of the ACM*, 59(2):64–73, 2016. 3
- [53] Pavel Tokmakov, Jie Li, Wolfram Burgard, and Adrien Gaidon. Learning to track with object permanence. In *Proceedings of the IEEE/CVF International Conference on Computer Vision*, pages 10860–10869, 2021. 3
- [54] Pavel Tokmakov, Allan Jabri, Jie Li, and Adrien Gaidon. Object permanence emerges in a random walk along memory. *arXiv preprint arXiv:2204.01784*, 2022.
- [55] Basile Van Hoorick, Pavel Tokmakov, Simon Stent, Jie Li, and Carl Vondrick. Tracking through containers and occluders in the wild. In *Proceedings of the IEEE/CVF Conference on Computer Vision and Pattern Recognition*, pages 13802–13812, 2023. 3
- [56] Ashish Vaswani, Noam Shazeer, Niki Parmar, Jakob Uszkoreit, Llion Jones, Aidan N Gomez, Łukasz Kaiser, and Illia Polosukhin. Attention is all you need. *Advances in neural information processing systems*, 30, 2017. 4
- [57] Paul Voigtlaender, Michael Krause, Aljosa Osep, Jonathon Luiten, Berin Balachandar Gnana Sekar, Andreas Geiger, and Bastian Leibe. Mots: Multi-object tracking and segmentation. In *Proceedings of the ieee/cvf conference on computer vision and pattern recognition*, pages 7942–7951, 2019. 1
- [58] Benjamin Wilson, William Qi, et al. Argoverse 2.0: Next generation datasets for self-driving perception and forecasting. In *NeurIPS Datasets and Benchmarks Track (Round 2)*, 2021. 2
- [59] Nicolai Wojke, Alex Bewley, and Dietrich Paulus. Simple online and realtime tracking with a deep association metric. In *2017 IEEE international conference on image processing (ICIP)*, pages 3645–3649. IEEE, 2017. 3
- [60] Jialian Wu, Jiale Cao, Liangchen Song, Yu Wang, Ming Yang, and Junsong Yuan. Track to detect and segment: An online multi-object tracker. In *Proceedings of the IEEE/CVF conference on computer vision and pattern recognition*, pages 12352–12361, 2021. 3
- [61] Fisher Yu, Haofeng Chen, Xin Wang, Wenqi Xian, Yingying Chen, Fangchen Liu, Vashisht Madhavan, and Trevor Darrell. Bdd100k: A diverse driving dataset for heterogeneous multitask learning. In *Proceedings of the IEEE/CVF conference on computer vision and pattern recognition*, pages 2636–2645, 2020. 1, 3, 4
- [62] Hang Zhao, Antonio Torralba, Lorenzo Torresani, and Zhicheng Yan. Hacs: Human action clips and segments dataset for recognition and temporal localization. In *Proceedings of the IEEE/CVF International Conference on Computer Vision*, pages 8668–8678, 2019. 3
- [63] Xingyi Zhou, Vladlen Koltun, and Philipp Krähenbühl. Tracking objects as points. *arXiv:2004.01177*, 2020. 3, 7, 9
- [64] Xingyi Zhou, Tianwei Yin, Vladlen Koltun, and Philipp Krähenbühl. Global tracking transformers. In *Proceedings of the IEEE/CVF Conference on Computer Vision and Pattern Recognition*, pages 8771–8780, 2022. 1, 3, 5, 6, 7, 8, 9, 10, 11
- [65] Yan Zhu, Yuandong Tian, Dimitris Metaxas, and Piotr Dollár. Semantic amodal segmentation. In *CVPR*, 2017. 2, 3, 6